Ren *et al. EURASIP Journal on Wireless Communications and Networking* (2016) 2016:182
DOI 10.1186/s13638-016-0681-6

EURASIP Journal on Wireless Communications and Networking

RESEARCH

Open Access

Joint interference estimation and cancellation for coherent frequency hopping multiple-access systems

Yinpeng Ren[1*], Zuyao Ni[2], Linling Kuang[2], Sheng Wu[2] and Jianhua Lu[1]

Abstract

In this paper, we propose an iterative detection algorithm that reconstructs and cancels the multiple-access interference jointly without the knowledge of hopping patterns of the interfering users for SFH/BPSK systems in an ad hoc scenario. Since users are asynchronous in this scenario, signal in one hop of the desired users is affected by partial signals in unaligned hops, called the interference fragments, of the interfering users. We address the interference model by defining a virtual user, which has the same hopping pattern as that of the desired user and contains the feature of the interfering fragments. Then, we derive the joint interference reconstruction and multiple-user detection (MUD) algorithm using the factor graph framework. Simulation results show that the performance of the proposed algorithm can be improved by up to 2 dB than that of the traditional single user detection (SUD) in AWGN at the packet error rate of 10^{-2} for a total of 8 users over 20 hopping frequencies, and an outstanding performance may also be achieved in the channel with Doppler.

Keywords: Ad hoc system, Frequency hopping, Joint detection algorithm, Multiple-access interference, Interference reconstruction and cancellation, Virtual user equivalent

1 Introduction

Frequency hopping (FH) is considered as a promising technique to provide robustness against interference in various scenarios such as ad hoc system in the airborne tactical network [1]. In an FH multiple-user system, a packet is divided into several hops, which are sent over different frequencies according to the hopping patterns generated pseudo-randomly. As all users share the same frequency set, the hops of different users may be sent in the same frequency at the same time, causing the multiple access interference (MAI), and leading to serious performance degradation when the number of users is large. Although the multiple-user detection (MUD) is usually employed to deal with the MAI, the challenge for applying MUD in an ad hoc network is the potential lack of coordination between nodes [1].

In recent years, there has been effective work on improving the performance of frequency hopping systems against MAI. In [2–5], it was focused on hybrid direct sequence (DS)/FH system, which uses unique spreading sequences to decrease MAI. In [6], MUD was proposed for FH/DPSK. Furthermore, iterative MUD detection with hard decision and soft decision was proposed for FH/MFSK in [7] and [8], respectively. Interference mitigation with an expectation maximization (EM) approach for BFSK was proposed for asynchronous slow frequency hopping (SFH) systems in [9, 10] and [11]. However, these contributions in [6–11] are studied for non-coherent demodulation. In [12], a kind of limited per-hop multiple-user detection (PH-MUD) algorithms, which chooses the single user detection (SUD) or the MUD according to the number of users hop by hop, was provided for slow frequency hopping/phase-shift keying (SFH/PSK) coherent synchronous frequency hopping system, and a feasible two-user PH-MUD algorithm was proposed in [13]. In [14], an MAI model taking both the hopping patterns and the phase offset into account was built, and the framework of symbol level iterative detection algorithm per chip (PC)-MUD was proposed for SFH/BPSK. Nevertheless, in

*Correspondence: ryp08@mails.tsinghua.edu.cn
[1] Department of Electronic Engineering,Tsinghua University, Beijing, China
Full list of author information is available at the end of the article

[12–14], it was assumed that the receiver has full knowledge of hopping patterns of all users. This assumption requires additional coordination among users and is usually appropriated for a base station (BS)-mobile station (MS) scenario.

In the scenario of an ad hoc network, a general assumption is that only the hopping patterns of the desired signal can be known at the receiver, while that of the interfering users are unknown [9]. The information which can be known by the receiver is that all users have the same modulation mode, the same hop length, and the same carrier frequency sets. The traditional SUD only aims to receive signal of the desired user and simply ignores all other interference. However, its performance is degraded significantly and sometimes fails. Although the PH-MUD can work well for synchronous frequency hopping systems, it may revert to PH-SUD without the knowledge of the hopping patterns and pilot signals of the interfering users. Similarly, the PC-MUD proposed in [14] may not work in this scenario as the MAI model is unknown. For the SFH/BPSK systems, to the best of our knowledge, there is no feasible MUD algorithm exists in the scenario of ad hoc network.

The main contributions of this paper are as follows: (1) presenting the virtual user equivalent to simplify the MAI model, which converts the uncertain of the hopping patterns of the interfering users to the uncertain of the signals of the virtual user and (2) proposing a joint interference reconstruction and multiple-user detection (MUD) algorithm using the factor graph framework. Since the pseudo-random hopping patterns are unknown except by the desired user, the received symbols of the desired user may be interfered in some partial hops by the symbols of other users, which are defined as interfering fragments in this paper. Although symbols in interfering fragments belong to different users, they all appear at the same time and frequency as the desired user. By splicing the interference fragments of the interfering users hop by hop, a virtual user with the same hopping patterns as that of the desired user is defined. Thus, the MAI can be expressed as a simple interference model between the desired user and the virtual user. According to the simplified MAI model, we propose an iterative detection algorithm with joint interference reconstruction and cancellation without the knowledge of hopping patterns of the interfering users for SFH/BPSK systems. By formulating a factor graph to represent the SFH/BPSK systems, symbols of the desired user and the virtual user and the structure of the virtual user can be estimated jointly through several iterations. The performance of the proposed algorithm is compared with that of the SUD, PH-MUD, and erasure detection (ED). Simulation results show that the proposed algorithm has a better performance compared with other classic methods, and an outstanding performance can also be achieved in the channel with Doppler.

This paper is organized as follows. Section 2 makes a description for the system and the model with the virtual user. The proposed joint detection algorithm for SFH/BPSK is presented in Section 3. Simulation results are given in Section 4, and at last, the conclusion is drawn in Section 5.

2 System description and model of the virtual user

In this section, the ad hoc frequency-hopping multiple-user system is presented, and the virtual user equivalent is proposed to simplify the multiple access interference model.

2.1 System description and multiple access interference model

We consider a coded frequency hopping system with K users and N frequencies in an ad hoc communication network. For each user, information bits $\boldsymbol{b}$ are encoded and interleaved into an L-bit packet $\boldsymbol{c}$. Finally, each packet is divided into D segments with the same length. Each segment with $P/2$ pilots inserted at each of the front and the end sides is transmitted as a hop in different frequencies according to the pseudo random hopping pattern, which is unique for each user. As the hopping patterns are non-orthogonal, MAI occurs whenever more than one user transmits in the same frequency at the same time. In asynchronous frequency hopping systems, interference may only appear partly in one hop of the desired user, while in synchronous frequency hopping systems, the signals of the interfering users affect that of the desired user in one whole hop.

Although BPSK is adopted in this paper, the proposed algorithm can be extended to general PSK. The lth received symbol of user k is given by

$$s_k[l] = e^{j\cdot \mathsf{map}(u_k[l])}, \tag{1}$$

where $u_k[l]$ is the transmitted symbol, $\mathsf{map}(u_k[l])$ is the phase of $u_k[l]$, and symbols in one hop with the length of $R = L/D + P$ are sent in one frequency randomly. The received signal is written as

$$r_k[l] = A_k e^{j\cdot(\mathsf{map}(u_k[l])+\theta_k[l])} + n_0, \tag{2}$$

where A_k denotes the amplitude of the received signal of user k, $\theta_k[l]$ denotes the phase offset, which is different in each hop for each user, with the uniform distribution of 0 to 2π, and n_0 denotes the complex additive white Gaussian noise (AWGN) with the variance of $\sigma^2 = N_0/2$. In the AWGN channel, A_k is constant in one packet and $\theta_k[l]$ is constant in one hop. But in the AWGN channel

with Doppler, $\theta_k[\,l]$ changes linearly and the phase of the l_hth symbol in the hth hop can be expressed as

$$\theta_k[\,l_h] = \theta_k[\,1_k] + \triangle\theta_k(l_h - 1), \tag{3}$$

where $\triangle\theta_k$ is the Doppler frequency offset for user k.

Without loss of generality, it is assumed that user 1 is the desired user. The received baseband signal of user 1 is given by

$$r_1[l] = \sum_{k=2}^{K} A_k \delta(\omega_1[\,l]\,, \omega_k[\,l]\,)\widetilde{s}_{l,k} + A_1 e^{j\cdot(\mathrm{map}(u_1[l])+\theta_1[l])} + n_0, \tag{4}$$

in terms of

$$\delta(m,n) = \begin{cases} 1, & m = n, \\ 0, & m \neq n, \end{cases} \tag{5}$$

where $\delta(m,n) = 1$ denotes the event that two users transmits in the same frequency at the same time and $\widetilde{s}_{l,k}$ is the interference from user k.

In ad hoc systems, signals may arrive at a different time. The baseband signal from an interfering user at the output of the matched filters can be written as the summation of two weighted consecutive interference symbols [9]

$$\begin{aligned} \widetilde{s}_{l,k} &= \frac{\triangle t_k}{T} I_{l-1,k} + (1 - \frac{\triangle t_k}{T}) I_{l,k} \\ &= \widetilde{I}_{l,k} + \widetilde{I}'_{l,k}, \end{aligned} \tag{6}$$

where

$$I_{l,k} = \exp\left[j \cdot (\mathrm{map}(u_k[\,l]\,) + \theta_k[\,l]\,)\right], \tag{7}$$

$$\widetilde{I}_{l,k} = \begin{cases} \frac{\triangle t_k}{T} I_{l-1,k}, & \frac{\triangle t_k}{T} \geq \frac{1}{2}, \\ (1 - \frac{\triangle t_k}{T}) I_{l,k}, & \frac{\triangle t_k}{T} < \frac{1}{2}, \end{cases} \tag{8}$$

and $\widetilde{I}'_{l,k} = \widetilde{s}_{l,k} - \widetilde{I}_{l,k}$, T denotes the symbol duration, $0 \leq \triangle t_k < T$ denotes the delay of the symbol of the kth user with respect to that of the desired signal. In (6), the asynchronous symbol can be considered as the summation of two synchronous symbols $\widetilde{I}_{l,k}$ and $\widetilde{I}'_{l,k}$, where $\widetilde{I}_{l,k}$ has higher amplitude. Then, the received baseband signal of user 1 can be rewritten as

$$\begin{aligned} r_1[\,l] = \sum_{k=2}^{K} A_k \delta(\omega_1[l], \omega_k[\,l]\,)\widetilde{I}_{l,k} + \sum_{k=2}^{K} A_k \delta(\omega_1[\,l]\,, \omega_k[\,l]\,)\widetilde{I}'_{l,k} \\ + A_1 e^{j\cdot(\mathrm{map}(u_1[l])+\theta_1[l])} + n_0. \end{aligned} \tag{9}$$

In the traditional SUD, both the first two terms of (9) are ignored, causing the performance loss. The estimation and cancellation of symbols in either of these two terms can reduce the interference from other users. Since $\triangle t_k$ is not easy to be estimated, we only deal with symbols in the first term in (9), and symbols in the second term with the lower amplitude are treated in the same way as that the SUD does. The weight coefficient caused by $\triangle t_k$ is considered as the channel coefficient; then, it is combined with the amplitude A_k. The simulation results verify that this treatment of the asynchronous interference can perform very well. The detection algorithm taking the second term into account may have better performance and will be studied in future work.

2.2 Virtual user equivalent

According to (9), MAI is the summation of signals of all interfering users, but the pseudo randomly hopping patterns of the interfering users are unknown, so the MAI is difficult to be estimated. In this section, we define a virtual user so as to estimate the signal of the interfering user. As shown in Fig. 1a, one hop of user 1 is interfered by three interfering fragments from three users. Since all users have the same hop length, one hop of the desired user can only be affected from the left and/or right of the hop partially. Although these collided symbols in interfering fragments are subordinated to different interfering

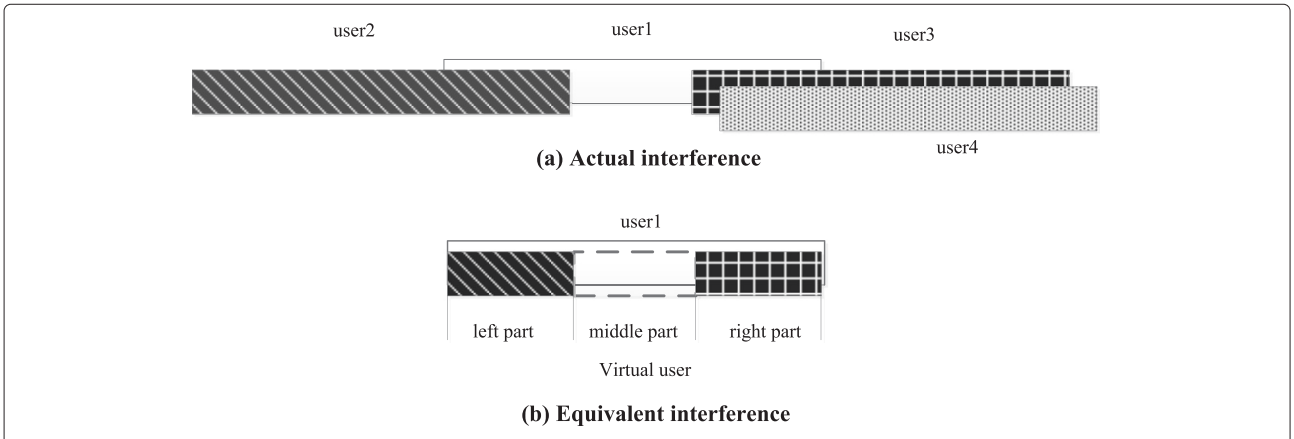

Fig. 1 General view of virtual user equivalent (**a**, **b**)

users, they are regarded as being sent from a special user, called the virtual user.

Assuming that there are K users' signals transmitted randomly over N frequencies, the probability of the symbols of the other i users interfering with that of the desired user is written as

$$P\left(i;K-1,\frac{1}{N-1}\right)=C_{K-1}^{i}\left(\frac{1}{N}\right)^{i}\left(\frac{N-1}{N}\right)^{K-i-1}, \tag{10}$$

and

$$\frac{P\left(i+1;K-1,\frac{1}{N-1}\right)}{P\left(i;K-1,\frac{1}{N-1}\right)}=\left(\frac{K}{i+1}-1\right)\frac{1}{N-1}. \tag{11}$$

If K is smaller than N, we have $P\left(1;K-1,\frac{1}{N-1}\right) > P\left(i;K-1,\frac{1}{N-1}\right)$, $\forall i = 2,3\cdots K$. Although the symbols of the desired user may be collided by that of more than one user, the probability is lower than that of being collided by that of only one user. The numerical results with $N = 20$ and different K is shown in Fig. 2. For a total of eight users, the probability of being collided by more than one user is lower than 0.1.

The virtual user has the same hopping pattern as that of the desired user and contains all symbols in interfering fragments, as shown in Fig. 1b. To describe the interference in one hop, the virtual user's signal contains three parts. The left part and the right part indicate the interference from left and right of the hop, respectively. The middle part, which represents symbols without interference, does not contain any symbol. The virtual signal, which is sent from the virtual user, in the hth hop is written as

$$s_{v,h}[\,l\,]=\begin{cases}A_{\mathrm{vh},h}e^{j\cdot\left[\mathrm{map}(u_{\mathrm{vh},h}[l])+\theta_{\mathrm{vh},h}\right]}, & 1\le l\le N_{\mathrm{head},h},\\ A_{\mathrm{vt},h}e^{j\cdot\left[\mathrm{map}(u_{\mathrm{vt},h}[l])+\theta_{\mathrm{vt},h}\right]}, & \left(R-N_{\mathrm{tail},h}\right)<l\le R,\\ 0, & \text{else},\end{cases} \tag{12}$$

where N_{head} and N_{tail} are the length of the left part and the right part and $u_{\mathrm{vh},h}[\,l\,]$ and $u_{\mathrm{vt},h}[\,l\,]$ are their signals. If there is no interference in the left (right) of the hop, $N_{\mathrm{head}} = 0$ ($N_{\mathrm{tail}} = 0$).

The virtual user is considered as user 2. Its phase offset is

$$\theta_{2,h}[\,l\,]=\begin{cases}\theta_{\mathrm{vh},h}, & 1\le l\le N_{\mathrm{head},h},\\ \theta_{\mathrm{vt},h}, & (R-N_{\mathrm{tail},h})<l\le R,\\ 0, & \text{else},\end{cases} \tag{13}$$

where θ_{vh} and θ_{vt} are the phase offset of the left part and the right part, respectively. There is phase ambiguity in the left and the right part because no pilot is available for the virtual user. The range of θ_{vh} and θ_{vt} is set to be $[\,0,\pi)$ to avoid the phase ambiguity. Interference in the synchronous frequency hopping systems is a special case with the signals in the whole hop is affected, the length of the right part is set to be 0, and the length of left part and the middle part is either 0 or R.

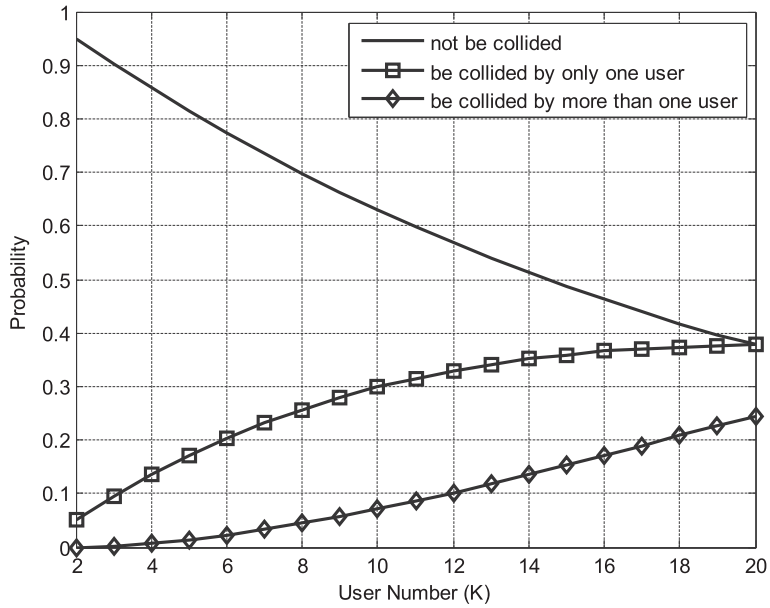

Fig. 2 Probability distribution of symbols with different K. $N = 20$

With the virtual user equivalent, the lth received signal of the desired user in the hth hop is rewritten as

$$r_{1,h}[\,l] = A_{1,h} \cdot e^{j\cdot[\mathrm{map}(u_{1,h}[l-hR])+\theta_{1,h}]} + s_{v,h}[\,l - hR]\, e^{j\theta_{2,h}[l]} + n_0, \tag{14}$$

where $hR \le l \le (h+1)R$. Then, the received signal can be expressed by the interference model

$$\begin{bmatrix} r_{1,h}[\,l] \\ r_{2,h}[\,l] \end{bmatrix} = \begin{bmatrix} e^{j\cdot\theta_{1,h}} & e^{j\cdot\theta_{2,h}} \\ e^{j\cdot\theta_{1,h}} & e^{j\cdot\theta_{2,h}} \end{bmatrix} \begin{bmatrix} A_{1,h}e^{j\mathrm{map}(u_{1,h}[l-hR])} \\ s_{v,h}[\,l - hR] \end{bmatrix} + n_0, \tag{15}$$

where the user 2 is the virtual user and $r_{2,h}[\,l] = r_{1,h}[\,l]$.

The MAI model in (15) shows that the virtual user equivalent converts the uncertain of the interference matrix and received signals of the interfering users to the uncertain of the signal of the virtual user. If the parameters of the virtual user are known, the symbols of the desired user and the virtual user can be detected jointly by the MUD. On the other hand, if we have the information of the symbols of the virtual user, the parameters of the virtual user can be estimated.

3 Interference cancellation algorithm

Using the simplified model in (15), a joint interference reconstruction and multiple-user detection algorithm is proposed in this section. The proposed interference cancellation algorithm consists of the detection of the symbols of the desired user and the virtual user by the MUD and the estimation of the parameters of the virtual user. The module of symbols detection is solved by the belief propagation (BP) algorithm [15, 16] in Section 3.1. Parameters of the virtual user are estimated in Section 3.2 with the prior information of signals of users, which is obtained from the iteration in the MUD, and the Cramer Rao Bound (CRB) derivations are also shown in this section. Then, the initialization of the parameters before iterations is presented in Section 3.3, and the summary of the proposed algorithm in both pseudo code implementation and schematic representation is shown at the end of this section.

3.1 Symbols detection

3.1.1 Detection module in the AWGN channel

In this part, we detect the symbols of the desired user by using the factor graph (FG) representation. The joint probability distribution can be factored into

$$\begin{aligned} &p(\boldsymbol{r}, \boldsymbol{b}_1, \boldsymbol{c}_1, \boldsymbol{u}_1, \boldsymbol{u}_2, \boldsymbol{\theta}_1, \boldsymbol{\theta}_{vh}, \boldsymbol{\theta}_{vt}) \\ =&p(\boldsymbol{b}_1)p(\boldsymbol{c}_1 \mid \boldsymbol{b}_1)p(\boldsymbol{r}, \boldsymbol{u}_1, \boldsymbol{u}_2, \boldsymbol{\theta}_1, \boldsymbol{\theta}_{vh}, \boldsymbol{\theta}_{vt} \mid \boldsymbol{c}_1) \\ =&p(\boldsymbol{b}_1)p(\boldsymbol{c}_1 \mid \boldsymbol{b}_1)p(\boldsymbol{u}_1 \mid \boldsymbol{c}_1)p(\boldsymbol{u}_2)p(\boldsymbol{\theta}_1)p(\boldsymbol{\theta}_{vh})p(\boldsymbol{\theta}_{vt}) \\ &\times \prod_{1\le h\le L/D, 1\le l\le R} f_j(r_{1,h}[\,l] \mid u_{1,h}[\,l]\,, u_{2,h}[\,l]\,, \theta_{1,h}, \theta_{vh,h}, \theta_{vt,h}), \end{aligned} \tag{16}$$

where $\boldsymbol{u}_2$ denotes the virtual signal and

$$f_j(r_{1,h}[\,l] \mid u_{1,h}[\,l]\,, u_{2,h}[\,l]\,, \theta_{1,h}, \theta_{\mathrm{vh},h}, \theta_{\mathrm{vt},h}) \propto \exp\left\{-\frac{\left[\mathcal{R}\left(r_{1,h}[\,l] - u_{1,h}[\,l]\, e^{j\theta_{1,h}[l]} - u_{2,h}[\,l]\, e^{j\theta_{2,h}[l]}\right)\right]^2}{2\sigma^2}\right\}, \tag{17}$$

where $u_{2,h}[\,l]\, e^{j\theta_{2,h}[l]} = s_{v,h}[\,l - hR]\, e^{j\theta_{2,h}[l]}$, and (17) will be expressed as $f_j(r_h[\,l] \mid \boldsymbol{u}_h[\,l]\,, \boldsymbol{\theta}_h[\,l]\,)$ for simplicity.

This factorization defined by (16) is represented by the factor graph in Fig. 3, where nodes with "=" in the factor graph represent the cloning of variable as in [15].

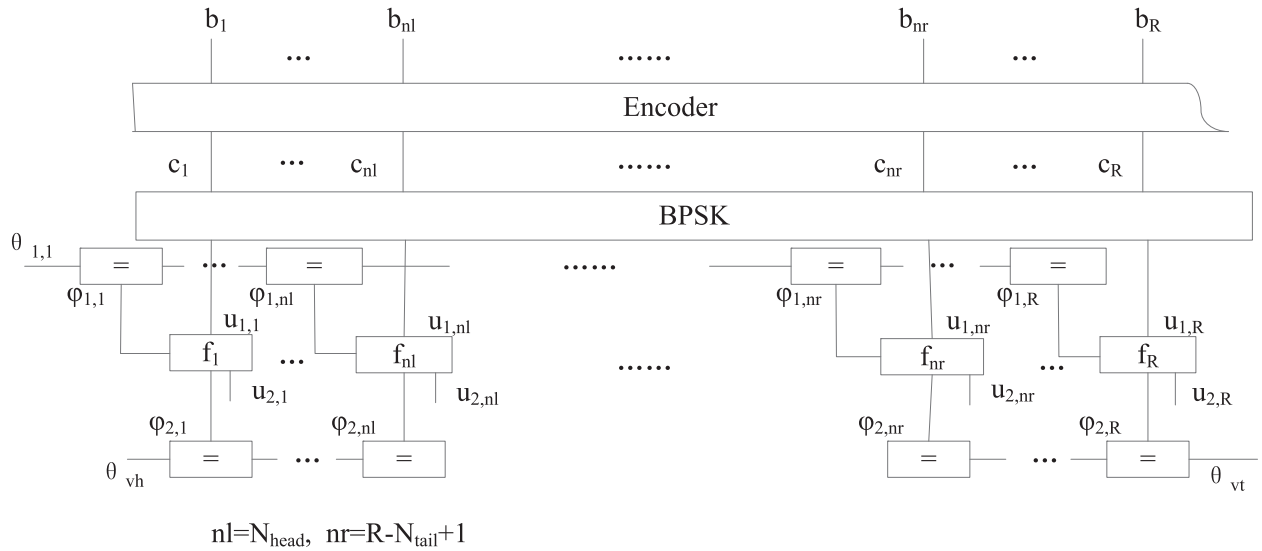

Fig. 3 Factor graph representation of the multiple-user FH system for one hop in AWGN. Note that the Turbo code is across all hops

Let $\mu_{a\to b}(b)$ denote the message sent from a to b. The message updating rules are

$$\mu_{f_l\to u_{i,l}}(u_{i,l}) = \sum_{u_{i',l},i'\neq i}\int_0^{2\pi}\int_0^{\pi} f_l\left(r_{1,h}[\,l\,]\mid \mathbf{u}_h[\,l\,],\varphi_h[\,l\,]\right) \times \mu_{\varphi_{2,l}\to f_l}\left(\varphi_{2,l}\right)\mu_{\varphi_{1,l}\to f_l}\left(\varphi_{1,l}\right)\mu_{u_{i',l}\to f_l}\left(u_{i',l}\right)d\varphi_{2,l}d\varphi_{1,l}, \tag{18}$$

$$\mu_{f_l\to\varphi_{i,l}}(\varphi_{i,l}) = \sum_{u_{i,l}}\sum_{u_{i',l},i'\neq i}\int_0^{\pi i} f_l\left(r_{1,h}[\,l\,]\mid \mathbf{u}_h[\,l\,],\varphi_h[\,l\,]\right) \times \mu_{\varphi_{i',l}\to f_l}(\varphi_{i',l})\mu_{u_{1,l}\to f_l}(u_{1,l})\mu_{u_{2,l}\to f_l}(u_{2,l})d\varphi_{i',l}, \tag{19}$$

$$\mu_{\varphi_{i,l}\to f_l}(\varphi_{i,l}) = \prod_{l'\neq l}\mu_{f_{l'}\to\varphi_{i,l'}}(\varphi_{i,l'}). \tag{20}$$

For the desired user, the message from node $u_{1,l}$ to f is the extrinsic information from the decoder. The $\mu_{\varphi_{1,l}\to f_l}(\varphi_{1,l})$ in (20) is the multiplications of $\left\{\mu_{f_{l'}\to\varphi_{1,l'}}(\varphi_{1,l'}), l'\neq l\right\}$ in one hop. Since the values of pilots are known, $\mu_{f_l\to\varphi_{1,l}}(\varphi_{1,l})$ with respect to the pilots is boiled down to

$$\mu_{f_l\to\varphi_{1,l}}(\varphi_{i,l}) = \sum_{u_{2,l}}\int_0^{\pi} f_l\left(r_{1,h}[\,l\,]\mid \mathbf{u}_h[\,l\,],\varphi_h[\,l\,]\right) \times \mu_{\varphi_{2,l}\to f_l}(\varphi_{2,l})\mu_{u_{2,l}\to f_l}(u_{2,l})d\varphi_{2,l}. \tag{21}$$

For the virtual user, the values of the virtual signal are taken from the set of $\{0,+1,-1\}$, which means no signal in the middle part and signal value $+1$ and signal value -1 in the other two parts, respectively. Since the virtual signal does not have a full forward error correction coding, we have $\mu_{u_{i,l}\to f_l}(u_{i,l}) = \mu_{f_l\to u_{i,l}}(u_{i,l})$. Symbols in different parts have different phases in one hop, so the multiple multiplication in (20) should not be calculated within a hop. Exploiting the characteristic of continuity of the interference, a hop is divided into several sub-hops. All symbols in a sub-hop are assumed to be belong to one part. Therefore, the part length is quantified as the summation of multiple lengths of sub-hops. Although this assumption brings quantization error to the part length, the message from multiple symbols can be used together to make more exact messages. Updating rule in (20) for the virtual user is calculated in a sub-hop with the length R_m. For the lth symbol in one hop, the multiplications in (20) start at symbol $l_s = \lfloor (l-1)/R_m\rfloor R_m + 1$ and end at symbol $l_e = (\lfloor (l-1)/R_m\rfloor + 1)R_m$, where $\lfloor\cdot\rfloor$ means the nearest integer toward 0.

Note that there are integral operations with respect to continuous random variables $\varphi_{1,l}$ and $\varphi_{2,l}$ in (18) and (19). Since the analytical expression for these two parameters is quite difficult to be obtained, the phase discretization discussed in [17] is employed. The phases are quantized at the values $e^{js\pi/(4M)}$, where $s = 8m+n$, $0\le m\le 1$ for $\varphi_{1,l}$ and $m=0$ for $\varphi_{2,l}$, and $0\le n\le 7$.

The interference from another user is shown in Fig. 4. It is supposed that the phase offset of user 1 is 0, and the other user has a phase offset of θ. The actual interference from the other user is the projection to the phase offset of user 1 at the point C or D. In order to simplify the calculation in (18) and (19), interference symbol from the interfering user is considered as a continuous random variable and the message is approximated into a real Gaussian random variable with a phase offset. The mean and the variance of the interference symbol can be calculated as

$$E = A(P_+ - P_-)\cos\theta, \tag{22}$$

$$\mathrm{Var} = 4P_+P_-A^2\cos^2\theta, \tag{23}$$

where P_+ denotes the probability of the symbol equal to 1, P_- denotes the opposite case, and A denotes the amplitude. Hard decision of phase offset is employed when the user performs as a interfering user.

Then, Eq. (17) can be rewritten as

$$f_l(r_h[\,l\,]\mid \boldsymbol{u}_h[\,l\,],\boldsymbol{\varphi}_h[\,l\,]) = \exp\left\{-\frac{\left[\mathcal{R}(r_{1,h}[\,l\,]\,e^{-j\varphi_{i,h}[l]} - E_{i',h}[\,l\,] - A_{i,h}[\,l\,]\,u_{i,h}[\,l\,])\right]^2}{2(\sigma^2+\mathrm{Var}_{i',h}[\,l\,])}\right\}, \tag{24}$$

where $E_{i',h}[\,l\,]$ and $\mathrm{Var}_{i',h}[\,l\,]$ are the mean and variance of the Gaussian function approximated from the signal of the user i'. The messages from f_l in (18) and (19) can be rewritten as

$$\mu_{f_l\to u_{i,l}}(u_{i,l}) = \sum_{\varphi_{i,l}}\mu_{\varphi_{i,l}\to f_l}(\varphi_{i,l})\cdot f_l\left(r_{1,h}[\,l\,]\mid \mathbf{u}_h[\,l\,],\varphi_h[\,l\,]\right), \tag{25}$$

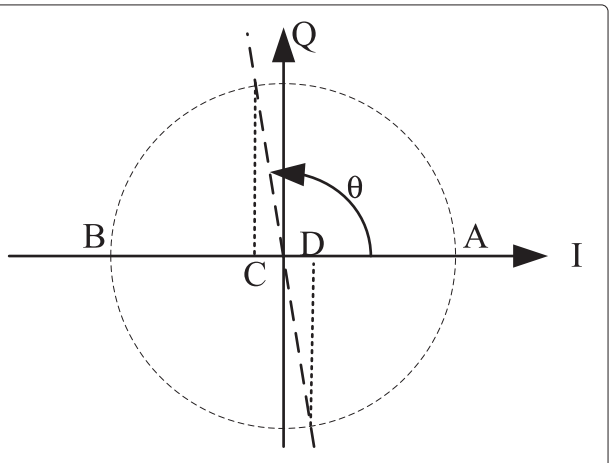

Fig. 4 Interference from another user with different phase offset

$$1\mu_{f_l\to\varphi_{i,l}}(\varphi_{i,l}) = \sum_{u_{i,h}[l]} \mu_{u_{i,l}\to f_l}(u_{i,l}) \cdot f_l\left(r_{1,h}[\,l] \mid \mathbf{u}_h[\,l], \varphi_h[\,l]\right). \tag{26}$$

Using the factor graph in Fig. 3 and update rules shown in (20), (25), and (26), the symbols of the desired user and the virtual user can be detected by using the BP algorithm.

3.1.2 Detection module in the AWGN channel with Doppler

In this part, we will discuss the detection module in the AWGN channel with Doppler, which makes the phase changing in a hop. Assuming that the Doppler is constant in one hop for all users, the difference of two phase offset between two symbols is $\Delta\theta$, where $\|\Delta\theta\|$ is usually a little value. For the lth symbol in one hop, phase of adjacent symbols are $\varphi_{i,l\pm1} = \varphi_{i,l} \pm \Delta\theta$.

However, message $\mu_{f_{l-1}\to\varphi_{i,l-1}}(\varphi_{i,l-1})\mu_{f_{l+1}\to\varphi_{i,l+1}}(\varphi_{i,l+1})$ can still be used for the phase estimation of the lth symbol without the information of $\Delta\theta$. For simplicity, we suppose that the symbol values have been obtained by the receiver, and all symbols have the same amplitude, rules (26) for adjacent symbols of symbol l are

$$\begin{aligned}&\mu_{f_{l-1}\to\varphi_{i,l-1}}(\varphi_{i,l-1} = \psi_{i,l} + \varsigma)\\ &= \exp\left\{-\frac{\left(\mathcal{R}(e^{j\varphi_{i,l-1}}e^{-j(\psi_{i,l}+\varsigma)} - 1)\right)^2}{2\sigma^2}\right\},\end{aligned} \tag{27}$$

$$\begin{aligned}&\mu_{f_{l+1}\to\varphi_{i,l+1}}(\varphi_{i,l+1} = \psi_{i,l} + \varsigma)\\ &= \exp\left\{-\frac{\left(\mathcal{R}(e^{j\varphi_{i,l+1}}e^{-j(\psi_{i,l}+\varsigma)} - 1)\right)^2}{2\sigma^2}\right\}.\end{aligned} \tag{28}$$

As a result, we have

$$\begin{aligned}&\mu_{f_{l-1}\to\varphi_{i,l-1}}(\varphi_{i,l-1} = \psi_{i,l} + \varsigma)\mu_{f_{l+1}\to\varphi_{i,l+1}}(\varphi_{i,l+1} = \psi_{i,l} + \varsigma)\\ &\propto -\frac{(\cos(\Delta\theta + \varsigma) - 1)^2 + (\cos(\Delta\theta - \varsigma) - 1)^2}{2\sigma^2}\\ &= -\frac{2 - 4\cos\Delta\theta\cos\varsigma + \cos^2(\Delta\theta + \varsigma) + \cos^2(\Delta\theta - \varsigma)}{2\sigma^2}\\ &= -\frac{3 - 4\cos\Delta\theta\cos\varsigma + \cos(2\Delta\theta)\cos(2\varsigma)}{2\sigma^2}\\ &= -\frac{2\cos(2\Delta\theta)\cos^2\varsigma - 4\cos\Delta\theta\cos\varsigma - \cos(2\Delta\theta) + 3}{2\sigma^2}\\ &= -\frac{2\cos(2\Delta\theta)\left(\cos\varsigma - \frac{\cos\Delta\theta}{\cos(2\Delta\theta)}\right)^2 + C}{2\sigma^2},\end{aligned} \tag{29}$$

where C is a constant. Since $\|\Delta\theta\|$ is a little value, $\cos\Delta\theta/\cos(2\Delta\theta) > 1$. The message achieves the maximum when $\varsigma = 0$. So the joint phase probability distribution of two symbols $l + i$ and $l - i$ can be used for estimating the phase of the lth symbol, which is the middle of these two symbols. Then, a sliding window is employed for the phase estimation. The length of the sliding window is $2R_m - 1$. For the desired user, the pilots should be used for $\mu_{\varphi_{i,l}\to f_l}(\varphi_{i,l})$ to avoid the phase ambiguity, and the range of $[\,l_s, l_e]$ for the $\prod\cdot$ in (20) for the lth symbol in one hop is

$$\begin{cases}[\,1, l + R_m - 1], & l < P/2 + R_m,\\ [\,1, P/2]\bigcup[\,l - R_m + 1, l + R_m - 1], & P/2 + R_m \le l < R/2,\\ [\,l - R_m + 1, l + R_m - 1]\bigcup[\,R - P/2, R], & R/2 \le l < R - P/2 - R_m,\\ [\,l - R_m + 1, R], & l \ge R - P/2 - R_m,\end{cases} \tag{30}$$

Note that for the virtual user, the $\prod\cdot$ in (20) starts at the symbol $\max(1, l - R_m - 1)$ and ends at the symbol $\min(l + R_m - 1, R)$.

3.2 Parameter estimation

The parameters of $s_{v,h}[\,l]$, which are considered to be fixed in the symbols detection module, are updated in this section. The received signal of the virtual user is

$$r_{2,h}[\,l] = s_{v,h}[\,l - hR] + n_0 + n_{\text{user}}, \tag{31}$$

where n_{user} is the interference from the desired user, which is approximated into a Gaussian random variable.

For the virtual user, if $u_{f_i\to u_{i,l}}(u_{i,l} = 0)$ is larger than $u_{f_i\to u_{i,l}}(u_{i,l} \neq 0)$, the received symbol of the desired user is nearer to 0 rather than to the BPSK constellation points. When $u_{f_i\to u_{i,l}}(u_{i,l} = 0)$ and $u_{f_i\to u_{i,l}}(u_{i,l} \neq 0)$ are close to each other, we prefer there is no signal existing to reduce the false alarm of the interference. Thus signal is decided to exist only if $\ln(u_{f_i\to u_{i,l}}(u_{i,l} \neq 0)) > \ln(u_{f_i\to u_{i,l}}(u_{i,l} = 0)) + \tau$, where τ is the decision threshold.

However, the accuracy of the decision using only one symbol is not high enough because of the interference and the noise. Since symbols in a sub-hop, which is defined in Section 3.1.1, belong to the same part, their messages can be used to make decision together. In a sub-hop, the probability distribution of symbols can be calculated as

$$f_{i,l}(u = 0) = \sum \ln(u_{f_i\to u_{i,l}}(u_{i,l} = 0)) + \tau R_m, \tag{32}$$

$$f_{i,l}(u \neq 0) = \sum \max_{u_{i,l}\neq 0}(\ln(u_{f_i\to u_{i,l}}(u_{i,l}))), \tag{33}$$

where the range of $\sum\cdot$ is the same as that of the sub-hop in Section 3.1.1.

Using the calculation in (32) and (33), each sub-hop has a decision for whether the interference signal exists independently. However, the decision results of all sub-hops may not correspond to that of three parts obviously in one hop. As indicated in Fig. 5, a sub-hop is shown with shadow if this sub-hop is decided to have signal. Sub-hops with different decision results may mix with others. So we cannot classify these sub-hops directly.

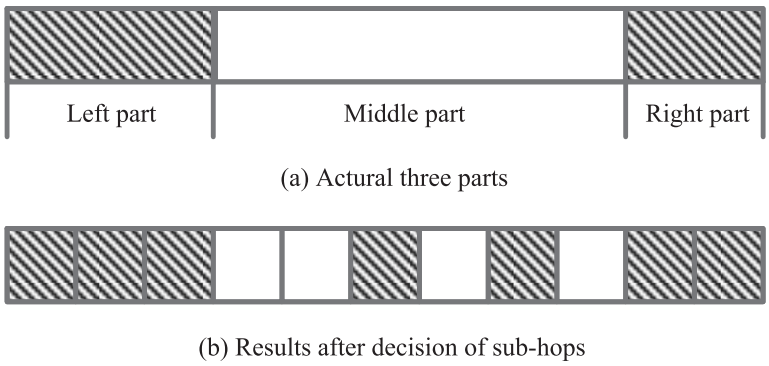

Fig. 5 Diagrammatic sketch of decision of the part length (**a**, **b**)

Since interferences can only appear at one side of one hop, the left part and the right part should start from the first and the last sub-hop, respectively, and end before the sub-hop without shadow. As is seen in the bottom of Fig. 5, the left part starts from the first sub-hop and ends at the third sub-hop and the right part is the last two sub-hops. Then, the remaining sub-hops are decided to belong to the middle part.

Using the lengths of three parts, the phase offsets of the virtual user in each hop can be estimated by

$$\theta_{v,h} = \prod_{l=1}^{N_{\text{head},h}} \mu_{f_l \to \varphi_{i,l}}(\varphi_{i,l}), \tag{34}$$

$$\theta_{v,t} = \prod_{l=R-N_{\text{tail},h}+1}^{R} \mu_{f_l \to \varphi_{i,l}}(\varphi_{i,l}), \tag{35}$$

and the amplitude of the virtual user in the hth hop is recalculated as follows

$$A_{\text{vh},h} = \frac{1}{N_{\text{head},h}} \sum_{l=hR}^{N_h} \left\| \mathcal{R}\left[(r_{1,h}[l] - \hat{u}_{1,h}[l]\, e^{j\hat{\theta}_{1,h}[l]}) e^{-j\hat{\theta}_{\text{vh},h}[l]} \right] \right\|, \tag{36}$$

$$A_{\text{vt},h} = \frac{1}{N_{\text{tail},h}} \sum_{l=N_t}^{(h+1)R} \left\| \mathcal{R}\left[(r_{1,h}[l] - \hat{u}_{1,h}[l]\, e^{j\hat{\theta}_{1,h}[l]}) e^{-j\hat{\theta}_{\text{vt},h}[l]} \right] \right\|, \tag{37}$$

where $\hat{u}_{1,h}[l]$, $\hat{\theta}_{1,h}[l]$, $\hat{\theta}_{\text{vh},h}[l]$, and $\hat{\theta}_{\text{vt},h}[l]$ are the hard decision of $u_{1,h}[l]$, $\theta_{1,h}[l]$, $\theta_{\text{vh},h}[l]$, and $\theta_{\text{vh},h}[l]$, $N_h = hR + N_{\text{head},h} - 1$ and $N_t = (h+1)R - N_{\text{tail},h} + 1$. Amplitude of symbols in the middle part are set to be 0. Then, the updated parameters are feedback to the module of interference estimation, leading to another new iteration.

In order to express a lower bound on the variance of parameters, the CRB [18] is given, which is used as the theoretical bound to evaluate the performance of practical estimation methods in many papers [19, 20]. Since the received signal contains symbols of both the desired user and the virtual user, the extrinsic information of the symbols of the desired user may affect the parameter estimation. If the symbols of the desired user are well detected in the symbol detection part, we can accurately estimate the parameters of the virtual user, or the mean square error (MSE) of estimation may increase. The lowest MSE bound may be achieved when we have information of the desired user. So the symbols of the desired user are assumed to be deterministic in the derivation.

The phase offset θ and the amplitude A of the virtual user are estimated after the determining of the lengths of three parts in a hop. We rewrite the received signal in (31) as

$$r = A\left(\cos(u+\theta) + j\sin(u+\theta)\right) + n_0, \tag{38}$$

where u denotes the phase of mapped symbols of the virtual user. Then, the joint probability density function is

$$f(r,\alpha) = \left(\frac{1}{\sigma^2 2\pi}\right)^N \times \exp\left\{ -\frac{1}{2\sigma^2} \sum_{n=0}^{N-1} \left[(\mathcal{R}(r_n) - A\cos(u+\theta))^2 + (\mathcal{I}(r_n) - A\sin(u+\theta))^2 \right] \right\}, \tag{39}$$

where $\alpha = [A, \theta]^T$ and N is the number of symbols in one part. The Fisher information matrix can then be derived as

$$[\mathbf{I}(\boldsymbol{\alpha})]_{1,1} = -E\left\{ \frac{\partial^2 \ln[f(r,\alpha)]}{\partial A^2} \right\} = \frac{N}{\sigma^2}, \tag{40}$$

$$[\mathbf{I}(\boldsymbol{\alpha})]_{1,2} = -E\left\{ \frac{\partial^2 \ln[f(r,\alpha)]}{\partial A \partial \theta} \right\} = 0, \tag{41}$$

$$[\mathbf{I}(\boldsymbol{\alpha})]_{2,1} = -E\left\{ \frac{\partial^2 \ln[f(r,\alpha)]}{\partial A \partial \theta} \right\} = 0, \tag{42}$$

$$[\mathbf{I}(\boldsymbol{\alpha})]_{1,2} = -E\left\{\frac{\partial^2 \ln[f(r,\alpha)]}{\partial\theta^2}\right\} = \frac{A^2N}{\sigma^2}. \tag{43}$$

Then, we can get the Fisher information matrix, i.e.,

$$\mathbf{I}(\boldsymbol{\alpha}) = \begin{bmatrix} \frac{N}{\sigma^2} & 0 \\ 0 & \frac{A^2N}{\sigma^2} \end{bmatrix}, \tag{44}$$

and the Cramer-Rao lower bound (CRLB) matrix is obtained by

$$\mathrm{CRLB} = [I(\alpha)]^{-1}, \tag{45}$$

where I^{-1} denotes the inverse of matrix I. Finally, the CRLB bounds can be written as

$$\mathrm{CRLB}(A) = \sigma^2/N, \tag{46}$$

$$\mathrm{CRLB}(\theta) = \sigma^2/\left(NA^2\right). \tag{47}$$

The MSE performances of parameter estimation are compared with the CRB bound and are shown in the simulation results.

3.3 Parameters initialization

Before the iterations between the symbol detection and the parameter estimation, some parameters should be initialized first.

After de-hopping, the received pilots is expressed as (14), where $hR \le l \le hR + P/2$ and $(h+1)R - P/2 \le l \le (h+1)R$. By correlating the received pilots with the transmitted pilots, we can perform the maximum-likelihood (ML) estimation. The results of the correlation for each hop is given by

$$\begin{aligned} A_{\mathrm{head},h} &= \tfrac{2}{P}\sum_{l=hR}^{hR+P/2-1} r_{1,h}[\,l]\cdot\exp\left(-j\cdot\mathrm{map}(u_1[\,l-hR]\,)\right), \\ A_{\mathrm{tail},h} &= \tfrac{2}{P}\sum_{l=(h+1)R-P/2+1}^{(h+1)R} r_{1,h}[l]\cdot\exp\left(-j\cdot\mathrm{map}(u_1[\,l-hR])\right). \end{aligned} \tag{48}$$

In the AWGN channel, the estimation of the amplitude of the desired user in a packet is

$$A_1 = \frac{1}{2D}\sum_{h=1}^{D}\left(\left\|A_{\mathrm{head},h} + A_{\mathrm{tail},h}\right\|\right), \tag{49}$$

Since the phase is constant in one hop, the initial value of the desired user is estimated as

$$\theta_{1,h} = \angle(A_{\mathrm{head},h} + A_{\mathrm{tail},h}). \tag{50}$$

The Doppler may cause considerable phase variation in one hop, so the initial value will be estimated by a linear interpolation. For the first half of symbols in one hop, we have

$$\theta_{\mathrm{head},h} = \frac{3}{4}\angle(A_{\mathrm{head},h}) + \frac{1}{4}\angle(A_{\mathrm{tail},h}), \tag{51}$$

and for the rest symbols in one hop,

$$\theta_{\mathrm{tail},h} = \frac{1}{4}\angle(A_{\mathrm{head},h}) + \frac{3}{4}\angle(A_{\mathrm{tail},h}). \tag{52}$$

With regard to the signal of the virtual user, the amplitude is constant in all three parts. Since there is no priori information at the beginning of the algorithm, N_{head} and N_{tail} are set to be $R/2$. The amplitudes of both parts on the hth hop are

$$A_{\mathrm{vh},h} = \left[\max\left(\tfrac{2}{R}\sum_{l=hR}^{N_h} r_{1,h}[l]\cdot\left(r_{1,h}[l]\right)^T - A_{1,h}^2 - \sigma^2, 0\right)\right]^{\frac{1}{2}}, \tag{53}$$

$$A_{\mathrm{vt},h} = \left[\max\left(\frac{2}{R}\sum_{l=N_t}^{(h+1)R} r_{1,h}[l]\cdot\left(r_{1,h}[\,l]\right)^T - A_{1,h}^2 - \sigma^2, 0\right)\right]^{\frac{1}{2}}. \tag{54}$$

The schematic representation of the proposed algorithm is shown in Fig. 6. The structure of successive interference cancellation is employed in the symbol detection module. Note that there is no decoder behind the detection for the virtual user because the signals of the

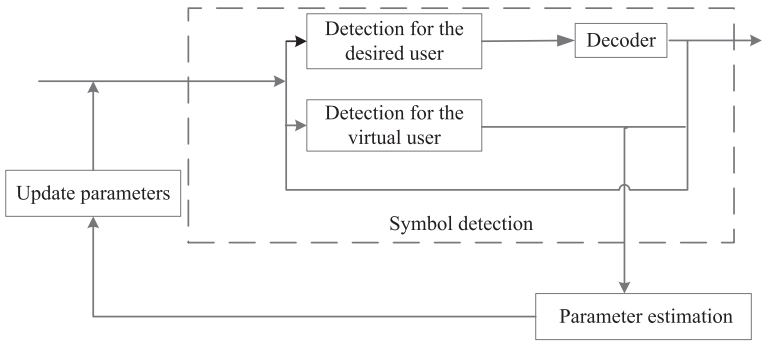

Fig. 6 The schematic representation of proposed algorithm

virtual user are spliced by different interfering users. For one iteration of the proposed algorithm, information of the desired user and the virtual user are obtained in the symbol detection module, then the parameters are estimated and updated by the parameter estimation module. The detailed algorithm is summarized in Table 1.

In the first iteration, there is no information of the phase of the virtual signal, so its interference to the desired user is set to be 0. In other words, the SUD is employed for the detection of the desired user in the first iteration. In [21], it is shown that one iteration of decoding for one global iteration of detecting can effective utilize the iterative structure of the decoder. The scheme of "one internal iteration per global iteration" is employed in the proposed algorithm.

4 Simulation results

In this section, numerical results of the proposed algorithm are presented. A rate 1/2 turbo code with generator $(13, 15)_8$ is employed; 2048 coded bits are interleaved using the random permutations for time diversity and divided into 32 64-length segments. Each hop contains a segment and 16 random pilots. The signal of each user is sent over 20 hopping frequencies using the pseudorandom hopping patterns. It is assumed that the receiver only knows the hopping patterns, pilots, and interleaver of the desired user.

Since the hopping patterns of the interfering users are unknown, the famous MUDs cannot be used directly in the scenario of an ad hoc network. For comparison, we employ the method of ED, which assumes that the receiver has the collision information and erasures all interfered symbols. In the simulations of the proposed algorithm, 30 global iterations are performed. And the performance of traditional SUD with 30 decoding iterations is shown for comparison. The energy overhead dedicated to pilots is counted within E_b/N_0.

First, we investigate the performance of the proposed joint detection algorithm in AWGN channel. The length of sub-hop is 8 and the decision threshold is 0.5. Then, simulation results for totally eight users with the proposed detection algorithms in synchronous frequency hopping

Table 1 Summary of proposed algorithm

if in AWGN without Doppler **then**
  $\forall h$, calculate $A_1, A_{\mathrm{vh},h}, A_{\mathrm{vt},h}, \theta_{1,h}$
end if
if in AWGN with Doppler **then**
  $\forall h$, calculate $A_{\mathrm{head},h}, A_{\mathrm{tail},h}, A_{\mathrm{vh},h}, A_{\mathrm{vt},h}, \theta_{1,h}$
end if
while $t \leq$ MaxIter **do**
  // Detection for the desired user:
  for $l = 1 \rightarrow R, h = 1 \rightarrow D$ **do**
    calculate $E_{2,h}[l], \mathrm{Var}_{2,h}[l], I_s, I_e$;
    $\mu_{f_l \rightarrow \varphi_{1,l}}(\varphi_{1,l}) = \sum_{u_{1,h}[l]} \mu_{u_{1,l} \rightarrow f_l}(u_{i,l}) \cdot f_l(r_{1,h}[l] | \mathbf{u}_h[l], \varphi_h[l])$;
    $\mu_{\varphi_{1,l} \rightarrow f_l}(\varphi_{1,l}) = \prod_{l' \neq l} \mu_{f_{l'} \rightarrow \varphi_{1,l'}}(\varphi_{1,l'})$;
    $\mu_{f_l \rightarrow u_{1,l}}(u_{1,l}) = \sum_{\varphi_{1,l}} \mu_{\varphi_{1,l} \rightarrow f_l}(\varphi_{1,l}) \cdot f_l(r_{1,h}[l] \mid \mathbf{u}_h[l], \varphi_h[l])$;
  end for
  Decoding the information bits of the desired user, generating the extrinsic information
  // Detection for the virtual user:
  for $l = 1 \rightarrow R, h = 1 \rightarrow D$ **do**
    calculate $E_{1,h}[l], \mathrm{Var}_{1,h}[l], I_s, I_e$;
    $\mu_{f_l \rightarrow \varphi_{2,l}}(\varphi_{2,l}) = \sum_{u_{2,h}[l]} \mu_{u_{2,l} \rightarrow f_l}(u_{i,l}) \cdot f_l(r_{1,h}[l] | \mathbf{u}_h[l], \varphi_h[l])$;
    $\mu_{\varphi_{2,l} \rightarrow f_l}(\varphi_{2,l}) = \prod_{l' \neq l} \mu_{f_{l'} \rightarrow \varphi_{2,l'}}(\varphi_{2,l'})$;
    $\mu_{f_l \rightarrow u_{2,l}}(u_{2,l}) = \sum_{\varphi_{2,l}} \mu_{\varphi_{2,l} \rightarrow f_l}(\varphi_{2,l}) \cdot f_l(r_{1,h}[l] \mid \mathbf{u}_h[l], \varphi_h[l])$;
    $\mu_{u_{2,l} \rightarrow f_l}(u_{2,l}) = \mu_{f_l \rightarrow u_{2,l}}(u_{2,l})$;
  end for
  // Parameter estimation module
  for $h = 1 \rightarrow D$ **do**
    for each sub-hop **do**
      $f_{i,l}(u = 0) = \sum \ln(u_{f_l \rightarrow u_{i,l}}(u_{i,l} = 0))$;
      $f_{i,l}(u \neq 0) = \tau R_m + \sum \max_{u_{i,l} \neq 0}(\ln(u_{f_l \rightarrow u_{i,l}}(u_{i,l})))$;
      decide $N_{\mathrm{head}}, N_{\mathrm{tail}}$
      update $A_{\mathrm{vh},h}, A_{\mathrm{vt},h}$;
    end for
  end for
end while

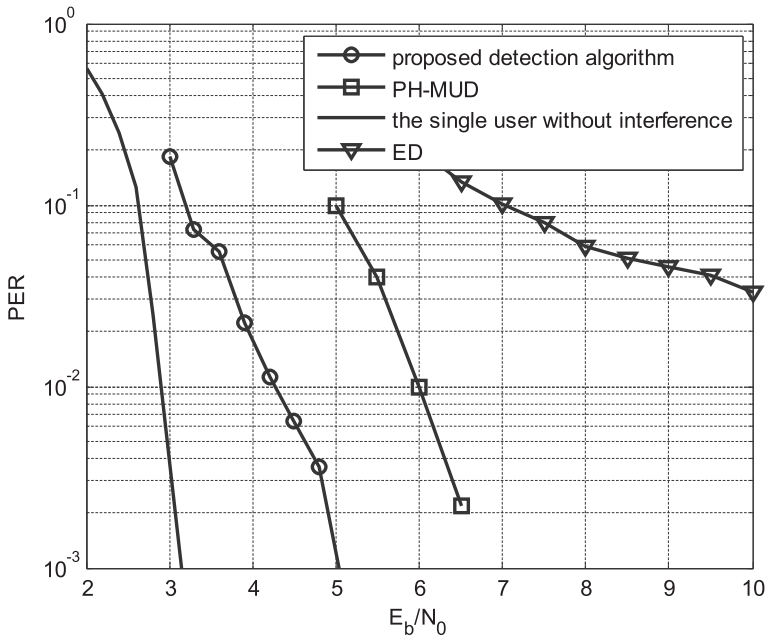

Fig. 7 Packet error rate performance for the proposed algorithm in AWGN in hopping synchronous systems. One packet contains 1024 information bits, and one hop has 64 symbols and 16 pilots. Power of each interfering user is 3 dB stronger than that of the desired user

systems are shown in Fig. 7. In this scenario, PH-MUD in [13] reverts to PH-SUD, which estimates the energy of the interference hop by hop. It is shown that the packet error rate (PER) of the ED is worse than that of the PH-MUD. However, the proposed algorithm achieves a gain of about 1.5 dB over the PH-MUD at the packet error rate of 1×10^{-2}.

The simulation results in the hopping asynchronous and symbol synchronous systems with 8, 4, and 2 users are shown in Fig. 8. The PER performances of SUD and ED

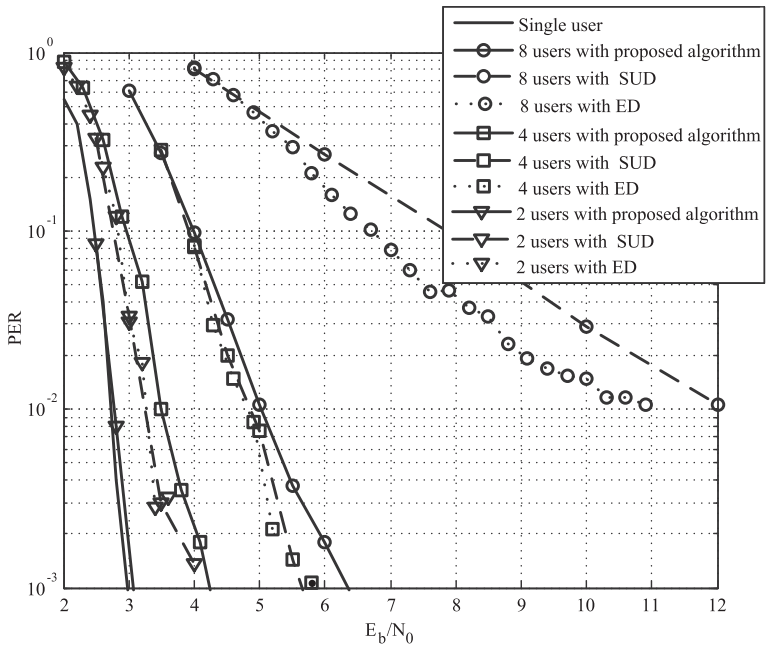

Fig. 8 PER for the proposed algorithm in AWGN in hopping asynchronous systems with synchronous symbols. One packet contains 1024 information bits, and one hop has 64 symbols and 16 pilots. Power of each interfering user is 3 dB stronger than that of the desired user. Data shown for SUD (*dashed*), proposed detection algorithm (*solid*), and totally 8 users (*circles*), 4 users (*squares*), and 2 users (*triangles*)

are also simulated. When user number is 2 or 4, the collided symbols are quite limited, so the performance of SUD and ED are almost coincident. The SUD without any information has worse performance than that of the ED when user number is 8. The performance of the proposed algorithm outperforms that of the SUD by 1 dB at the PER of 10^{-3} for totally 2 users. While for totally 4 users, this improvement is 2 dB. For 8 users, the simulation results show that the PER of SUD reach 1×10^{-2} when the E_b/N_0 is 12 dB. Although the performance of the ED performs a little better, it has a long distance to the performance of proposed algorithm, which achieves 1×10^{-3} at 6.5 dB. At the PER of 10^{-2}, the performance of the proposed algorithm is improved by up to 7 dB than that of SUD. Since the virtual user is an approximate equivalent of the interfering users, the proposed algorithm is not able to cancel all interferences. The distance to that of the single user without interference is 3.5 dB for 8 users over 20 hopping frequencies.

The simulation results for the condition of hopping asynchronous and symbol asynchronous are shown in Fig. 9. The delay between symbols of different users are random variables which obey uniform distribution within a symbol duration. The PER performances of the proposed algorithm and SUD are presented when the power of interfering users is 3 and 6 dB stronger than that of the desired user, respectively. And the PER performance of the ED is also shown. Since the ED only erasures the interfering symbols, it is not affected by the power of interfering users. The PER performance of ED is better than that of SUD with 6 dB MAI, but worse than that of SUD with 3 dB MAI. The SUD can achieve the PER of 1×10^{-2} at the E_b/N_0 of 6.5 dB with the 3 dB higher interfering users, and the proposed algorithm achieves a gain of about 2 dB over the SUD. Under a higher MAI that the power of each interference user is 6 dB stronger than that of the desired user, the performance of SUD is only 10^{-1} at the E_b/N_0 of 13 dB, while the proposed algorithm shows its outstanding performance and can achieve the PER of 1×10^{-2} at the E_b/N_0 of 6.3 dB.

We then study the parameters of the proposed algorithm in asynchronous hopping system. Different values of the length of sub-hop R_m and the decision threshold τ are adopted in the simulations, respectively. The user number is set to be 8.

In Fig. 10, simulation results are shown with different length of sub-hops, which are set to be 4, 8, and 16, respectively. It is shown that the algorithms with $R_m = 8$ is better than that with $R_m = 4$ and $R_m = 16$. As discussed in Section 3.1.1, the definition of sub-hops can exchange message among symbols with the same phase. However, it quantifies the length of three parts of the signal in one hop and introduces quantization error. A short R_m can reduce the quantization error but also reduce the accuracy of phase estimation. And a long R_m may increase the quantization error and

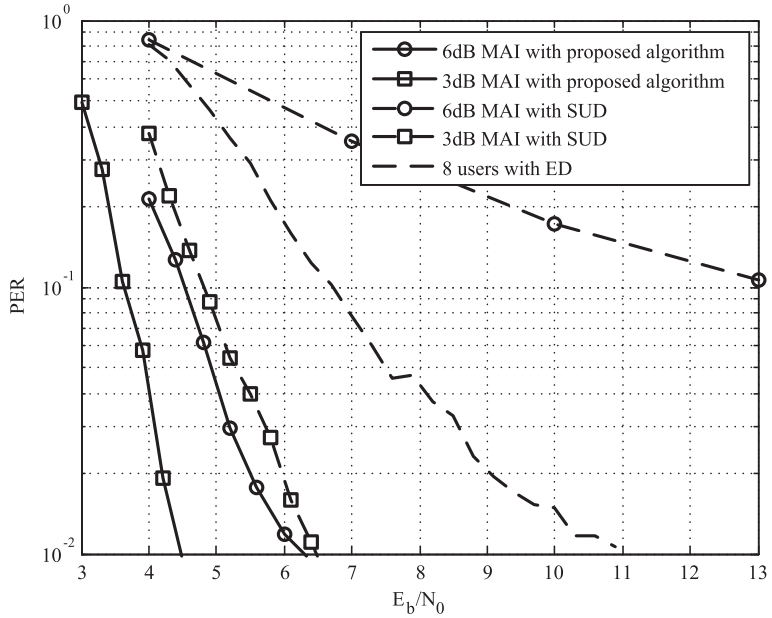

Fig. 9 PER for the proposed algorithm in AWGN in hopping asynchronous systems with asynchronous symbols. One packet contains 1024 information bits and one hop has 64 symbols and 16 pilots. Power of each interfering user is 3 dB (*squares*) or 6 dB (*circles*) stronger than that of the desired user. Data shown for SUD (*dashed*) and proposed detection algorithm (*solid*)

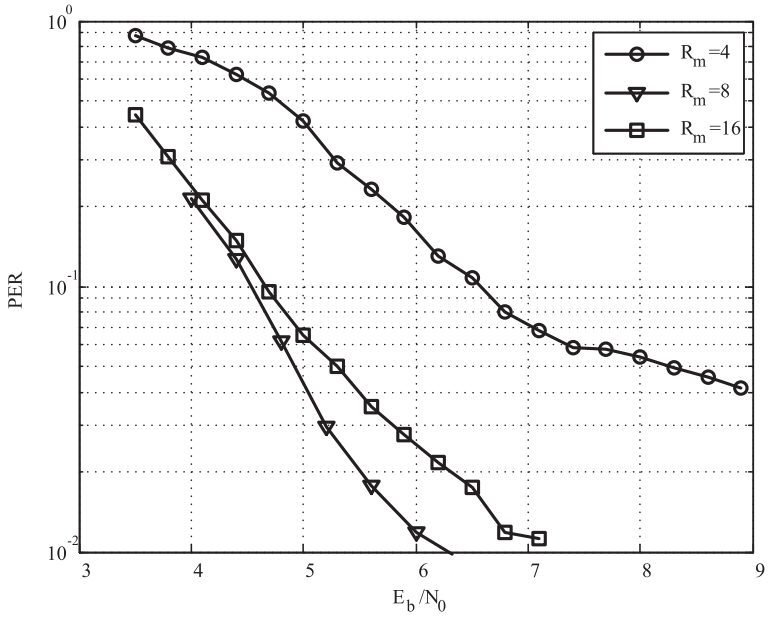

Fig. 10 PER with different length of sub-hops in AWGN in hopping asynchronous systems with asynchronous symbols. One packet contains 1024 information bits, and one hop has 64 symbols and 16 pilots. Power of each interfering user is 6 dB stronger than that of the desired user

the accuracy of phase estimation simultaneously. Suitable setting of the length of sub-hop can make a better performance.

Simulation results of the proposed algorithm with different τ , which is set to be 0, 0.5, 0.75, and 100, are shown in Fig. 11. For $\tau \leq 0.5$, the increase of τ can improve the detection performance. However, when τ is set to be 0.75, its performance is surpassed by that with $\tau = 0.5$. Since the decision threshold τ is defined to counteract the false alarm of interfering users caused by the noise and interference, the best τ depends on the energy of the noise. For a lower τ, the algorithm may

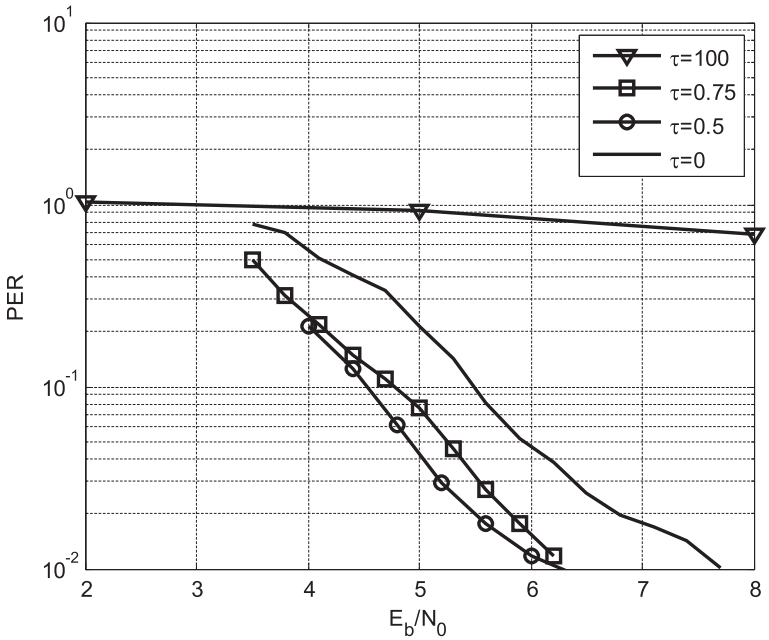

Fig. 11 PER with different decision threshold in AWGN in hopping asynchronous systems with asynchronous symbols. One packet contains 1024 information bits, and one hop has 64 symbols and 16 pilots. Power of each interfering user is 6 dB stronger than that of the desired user

work well without noise, but the false-alarm makes performance decline in the E_b/N_0 region used for simulations. For a higher τ, such as 0.75, it may suit for the low E_b/N_0 region, but cause missed alarm of interfering users for the high E_b/N_0 region. When τ is 100, it is large enough that $f_{i,l}(u = 0)$ in (32) is always smaller than $f_{i,l}(u \neq 0)$ in (33), the length of the left part and the right part in all hops are 0. Then, the proposed algorithm reverts to SUD, and its performance is even worse than SUD in Fig. 8 because of the approximation in the proposed detection algorithm.

Then, we simulate the proposed algorithm in AWGN with Doppler, which is assumed to be 0.4° per symbol for all eight users. Simulation results in Fig. 12 show that the proposed algorithm can work well for the environment with relative velocity between communication nodes. The E_b/N_0 required for the PER of 1×10^{-2} is about 4 dB higher than that without Doppler.

The MSE performance of the parameter estimation part is also considered in the ad hoc system with hopping asynchronous and symbol asynchronous. There are totally eight users. The power of each interfering user is 6 dB stronger than that of the desired user. The MSE performances of the estimated parameters of the virtual user, θ and A, are calculated at the final iteration and compared with the CRLBs, which are derived in Section 3.2. We classify the estimated parameters according to the length of three parts, which is different for each hop. The results are shown in Figs. 13 and 14, with the part length of 16 symbols (2 sub-hops) and 40 symbols (5 sub-hops). The CRLB curves are shown by dashed lines, and the MSEs of the proposed algorithm are shown by solid lines. The MSE performances of the estimation of both parameters θ and A degared as the noise energy decreases; however, they still keep a distance to the CRLB because of the incompletely accurate extrinsic information. For the parameter θ, the CRLB(θ) is lower than the MSE of the proposed algorithm by a order of magnitude. For the parameter A, the MSE is about twice higher than the CRLB(A). Although the estimation performance of the virtual user is not very accurate, it can help us to reconstruct the signal of the virtual user and reduce the MAI, leading to a higher success rate in the decoding process.

5 Conclusions

In this paper, we focus on the multiple-user interference reconstruction and cancellation in ad hoc frequency-hopping multiple-user systems without the knowledge of undesired interfering users. A virtual user which interferes with the signal of the desired user standing for all interfering fragments is defined, and a joint detection algorithm is integrated with factor graphs framework.

Simulation results show that an outstanding performance can be achieved by the proposed algorithm in scenarios of hopping synchronous and hopping asynchronous with both symbol synchronous and symbol asynchronous. The proposed algorithm is also robust to the environment with relative velocity between

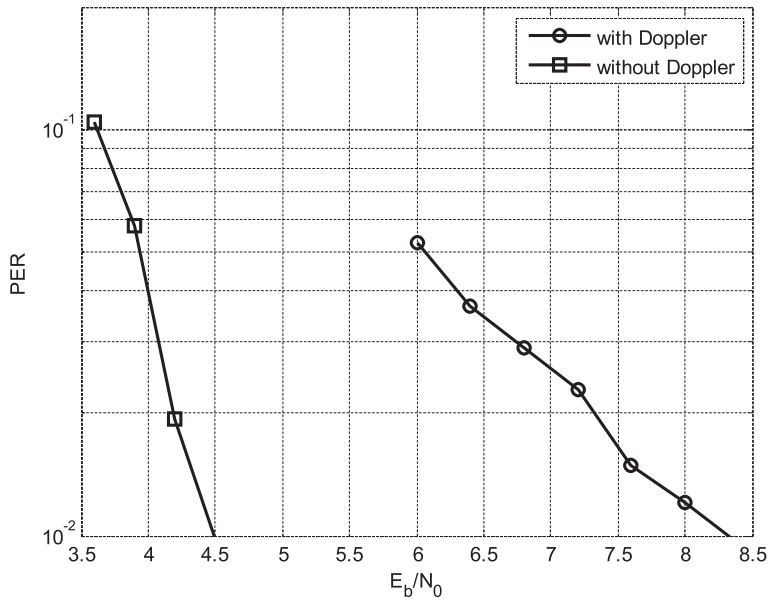

Fig. 12 PER with the proposed detection algorithm in AWGN with Doppler in hopping asynchronous systems with asynchronous symbols. One packet contains 1024 information bits, and one hop has 64 symbols and 16 pilots. Power of each interfering user is 3 dB stronger than that of the desired user

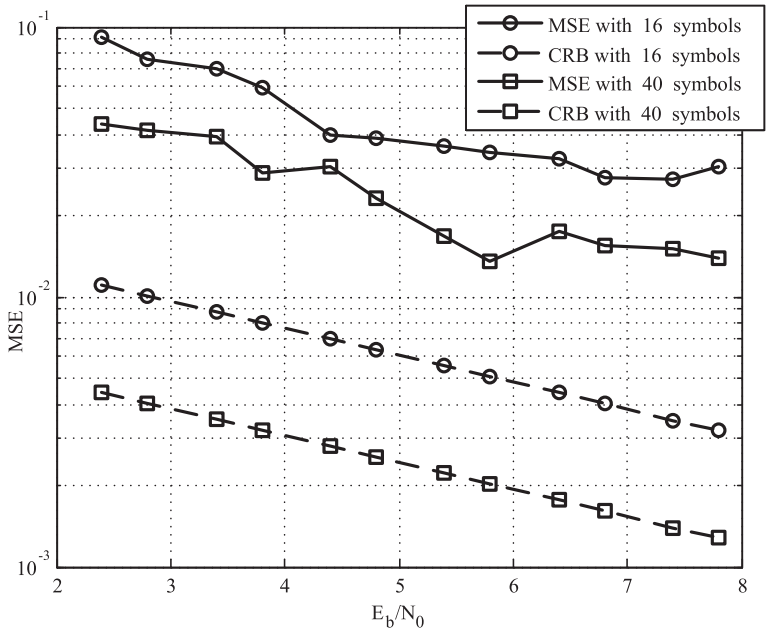

Fig. 13 MSE performance and CRLB of the parameter θ of the virtual user in the ad hoc system with hopping asynchronous and symbol asynchronous

communication nodes. Power of each interfering user is set to be 3 dB stronger than that of the desired user. The proposed algorithm can make a performance improvement of 1.5 dB in synchronous frequency hopping systems than that of PH-MUD at the packet error rate of 10^{-2} in AWGN. In asynchronous frequency hopping systems, the performance improvement is 7 dB with synchronous symbols and 2 dB with asynchronous symbols. And the proposed algorithm can also work well with the condition of Doppler.

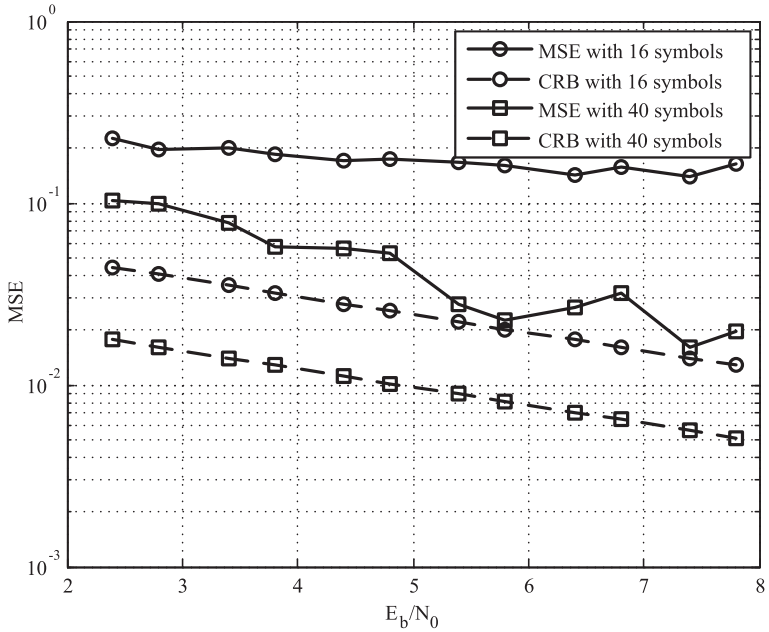

Fig. 14 MSE performance and CRLB of the parameter *A* of the virtual user in the ad hoc system with hopping asynchronous and symbol asynchronous

Acknowledgements
This work is partially supported by National Basic Research Program of China (2013CB329001), National Natural Science Foundation of China (91338101, 91338108), and Tsinghua University Initiative Scientific Research Program (20131089219).

Competing interests
The authors declare that they have no competing interests.

Author details
[1]Department of Electronic Engineering,Tsinghua University, Beijing, China.
[2]Tsinghua Space Center, Tsinghua University, Beijing, China.

Received: 17 November 2015 Accepted: 29 July 2016
Published online: 08 August 2016

References

1. B-N Cheng, FJ Block, BR Hamilton, D Ripplinger, C Timmerman, L Veytser, A Narula-Tam, Design considerations for next-generation airborne tactical networks. IEEE Commun. Mag. **52**(5), 138–145 (2014). doi:10.1109/MCOM.2014.6815904
2. JH Kim, SW Kim, Partial successive interference cancellation in hybrid DS/FH spread-spectrum multiple-access systems. IEEE Trans. Commun. **49**(10), 1710–1714 (2001). doi:10.1109/26.957390
3. MAR Khan, SD Rong, in *Proc. IEEE Multitopic Conference (INMIC '2006)*. Sensitivity analysis of hybrid DS/FH spread spectrum communication system capacity, (2006), pp. 47–51. doi:10.1109/INMIC.2006.358134
4. M Abou Eldahab, MA Nassar, M Fouad, AEM Mokhtar, in *Proc.11th Mediterranean Electrotechnical Conference (MELECON 2002)*. Coherent hybrid DS/SFH-SSMA micro and macro cellular communication, (2002), pp. 352–357. doi:10.1109/MELECON.2002.1014589
5. M Sakr, A Al-Moghazy, H Abou-Bakr, M Fikri, in *Proc. 2012 Japan-Egypt Conference on Electronics, Communications and Computers (JEC-ECC)*. Hybrid DS-FH packet acquisition for frequency hopped random multiple access, (2012), pp. 133–137. doi:10.1109/JEC-ECC.2012.6186971
6. D Qiu, FJ Block, in *Proc. 2013 51st Annual Allerton Conference on Communication, Control, and Computing (Allerton)*. Non-coherent multi-user detection of DPSK signals after differential demodulation, (2013), pp. 1052–1058. doi:10.1109/Allerton.2013.6736641
7. N Sharma, H El Gamal, E Geraniotis, Multiuser demodulation and iterative decoding for frequency-hopped networks. IEEE Trans. Commun. **49**, 1437–1446 (2001)
8. N Sharma, EA Geraniotis, Soft multiuser demodulation and decoding for FH/SSMA with a block turbo code. IEEE Trans. Commun. **51**, 1561–1570 (2003)
9. X Tan, JM Shea, An EM approach to multiple-access interference mitigation in asynchronous slow FHSS systems. IEEE Trans. Wireless Commun. **7**(7), 2661–2670 (2008)
10. OA Adeladan, JM Shea, in *Proc. 2009 IEEE Military Communications Conference (MILCOM 2009)*. Interference mitigation with partially coherent demodulation in a slow frequency-hopping spread-spectrum system, (2009), pp. 1–7. doi:10.1109/MILCOM.2009.5379989
11. OA Adeladan, JM Shea, in *Proc.2013 IEEE Military Communications Conference (MILCOM 2013)*. Multiple-access interference mitigation and iterative demodulation of CPFSK in asynchronous slow FHSS systems, (2013), pp. 1581–1586. doi:10.1109/MILCOM.2013.196
12. FJ Block, M Moore, D Qiu, TC Royster, in *2013 IEEE Aerospace Conference*. Frequency-hop multiple-access systems with limited per-hop multi-user detection, (Big Sky, MT, 2013), pp. 1–7. doi:10.1109/AERO.2013.6497130
13. D Qiu, Tc Royster, FJ Block, in *2013 51st Annual Allerton Conference on Communication, Control, and Computing (Allerton)*. Phase and power estimation for per-hop multi-user detection in frequency-hopping systems, (Monticello, IL, 2013), pp. 1045–1051. doi:10.1109/Allerton.2013.6736640
14. Y Ren, Z Ni, L Kuang, J Lu, in *2015 IEEE 82nd Vehicular Technology Conference (VTC Fall)*. Per-chip multi-user detection for SFH/BPSK systems, (Boston, MA, 2015), pp. 1–5. doi:10.1109/VTCFall.2015.7391067
15. H-A Loeliger, An introduction to factor graphs. IEEE Signal Process. Mag. **21**(1), 28–41 (2004). doi:10.1109/MSP.2004.1267047
16. JGD Forney, Codes on graphs: normal realizations. IEEE Trans. Inf. Theory. **47**(2), 520–548 (2001). doi:10.1109/18.910573
17. WG Phoel, Iterative demodulation and decoding of frequency-hopped PSK in partial-band jamming. IEEE J. Sel. Areas Commun. **23**(5), 1026–1033 (2005). doi:10.1109/JSAC.2005.845414
18. SM Kay, *Fundamentals of statistical signal processing, volumn I: estimation theory*. (Prentice-Hall, New Jersey, USA, 1993)
19. L Dai, Z Wang, Z Yang, Spectrally efficient time-frequency training OFDM for mobile large-scale mimo systems. IEEE J. Sel. Areas Commun. **31**(2), 251–263 (2013)
20. Z Deng, M Fu, S Jin, Y Zhang, Z Wang, Joint estimation of motion parameters using Newton's method. IEEE Trans. Aerosp. Electron. Syst. **51**(4), 3386–3398 (2015)
21. N Gu, S Wu, L Kuang, Z Ni, J Lu, Belief propagation-based joint iterative algorithm for detection and decoding in asynchronous CDMA satellite systems. EURASIP J. Wireless Commun. Netw. **2013**(1), 1–14 (2013). doi:10.1186/1687-1499-2013-234